Topographic–Isostatic Reduction of GOCE Gravity Gradients

Thomas Grombein, Kurt Seitz, and Bernhard Heck

Abstract

Gravity gradients measured by ESA's satellite mission GOCE (Gravity field and steady-state Ocean Circulation Explorer) are highly sensitive to mass anomalies and mass transports in the Earth system. The high and mid-frequency gradient components are mainly affected by the attraction of the Earth's topographic and isostatic masses. Due to these signal components, interpolation and prediction tasks, such as a harmonic downward continuation of the gradients, can be considered as ill-conditioned processes. One approach to mitigate the resulting instability is to smooth the observed gradients by applying topographic–isostatic reductions using a Remove–Compute–Restore technique.

This paper presents a reduction concept based on the developed Rock–Water–Ice decomposition in which the topography is represented by a vertical three-layer model with variable density values. Geometry and density information is derived from the topographic data base DTM2006.0. Furthermore, the Airy–Heiskanen isostatic model is adapted to the Rock–Water–Ice approach and extended by including a depth model for the Mohorovičić discontinuity obtained from the global crust model CRUST 2.0. Since these data are provided in geographical coordinates, tesseroid bodies that are arranged on an ellipsoidal reference surface are used for mass discretization.

The topographic–isostatic reduction values calculated along the orbit of the GOCE satellite reach a maximum of about 1 E (Eötvös unit, $1\,\mathrm{E} = 10^{-9}\,\mathrm{s}^{-2}$) and lead to significant smoothing effects on gradient measurements, particularly in regions with highly variable topography. Taking one week of real GOCE measurements as example, the degree of smoothing is analyzed, showing a significant reduction of the standard deviation (about 30 %) and the range (about 20–40 %).

Keywords

Topographic–isostatic reduction • Forward modelling • Rock–Water–Ice decomposition • Tesseroid • Satellite gravity gradiometry • GOCE

1 Introduction

Analysing gravity gradients measured by the GOCE satellite, high and mid-frequency signals can be detected which are mainly caused by the attraction of the Earth's topographic and isostatic masses. Due to the induced rough measurement

T. Grombein (✉) • K. Seitz • B. Heck
Geodetic Institute, Karlsruhe Institute of Technology (KIT),
Englerstr. 7, Karlsruhe 76128, Germany
e-mail: grombein@kit.edu

C. Rizos and P. Willis (eds.), *Earth on the Edge: Science for a Sustainable Planet*, International Association of Geodesy Symposia 139, DOI 10.1007/978-3-642-37222-3_46,

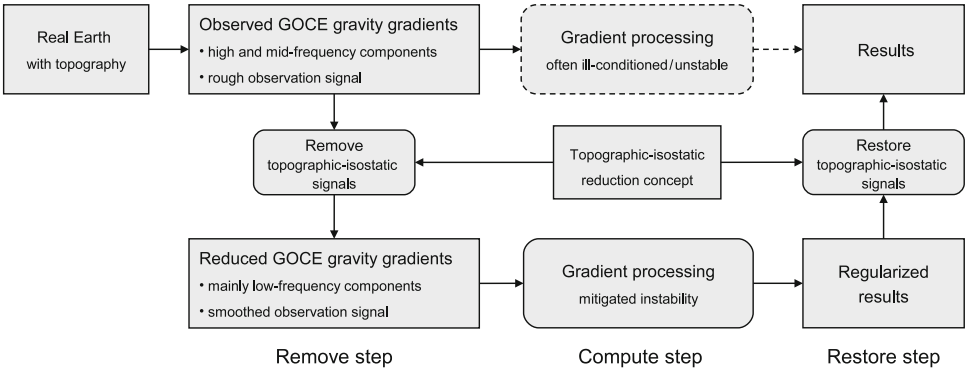

Fig. 1 Use of topographic–isostatic reductions in a Remove–Compute–Restore concept

signal, interpolation and prediction tasks performed with these gradients are often ill-posed problems. For instance, in the context of gravity field modelling, the harmonic downward continuation of the gradients from satellite altitude to Mean Sea Level (MSL) is an unstable process. For improving the numerical stability it is recommended to embed such problems in a Remove–Compute–Restore concept (Forsberg and Tscherning 1997), schematically shown in Fig. 1. In the remove step, topographic–isostatic signals are reduced in order to obtain a regularized gravity field mainly consisting of low-frequency components and smoothed gradient signals. In the compute step, interpolation and prediction tasks as well as field transformations can be carried out. The computations benefit from the improved stability and produce regularized results. In the restore step, consistent topographic–isostatic signals are reconsidered to obtain the final results. Previous investigations based on simulated GOCE gravity gradients have already shown that significant smoothing effects are possible (e.g. Wild and Heck 2008; Wild-Pfeiffer 2008; Janák et al. 2012). A closed loop simulation presented in Janák and Wild-Pfeiffer (2010) has verified the benefit of topographic–isostatic reductions for the downward continuation process.

In this paper, real GOCE gravity gradient measurements are smoothed by means of topographic–isostatic reductions relying upon a newly developed and advanced concept. Section 2 focuses on the used input data and the improved reduction concept is described in detail. In Sect. 3, results from numerical investigations are presented and discussed, along with an analysis of the smoothing potential for a reduced GOCE data set. Finally, Sect. 4 provides concluding remarks with an outlook for future research work.

2 Topographic–Isostatic Reduction Concept

Topographic–isostatic reductions can be obtained by forward modelling based on the evaluation of functionals of Newton's integral (Heiskanen and Moritz 1967, p. 3) extending over the domain of the Earth's topographic and isostatic masses Ω_{TI}:

$$V(x_1, x_2, x_3) = G \iiint_{\Omega_{\mathrm{TI}}} \frac{\rho(x_1', x_2', x_3')}{\ell} \, \mathrm{d}\Omega_{\mathrm{TI}}, \tag{1}$$

where G denotes Newton's gravitational constant, ρ the location-dependent density function, and ℓ the Euclidean distance between the attracted computation point $P(x_1, x_2, x_3)$ and the running integration point $Q(x_1', x_2', x_3')$. Thereby, global information on the geometry and mass density distribution of the Earth's crust and upper mantle is required, which have to be defined by a topographic model and an isostatic concept. According to the grid resolution of the used models, a mass discretization of the integration domain Ω_{TI} into elementary bodies with constant density values is performed. The decomposition is carried out using tesseroid bodies which are bounded by the grid lines of geographical coordinates and constant heights (Anderson 1976; Heck and Seitz 2007). In view of precision and computation time, previous studies have verified the high numerical efficiency when utilizing tesseroids instead of conventional rectangular prisms (Heck and Seitz 2007; Wild-Pfeiffer 2008; Grombein et al. 2010).

To determine the impact on gravity gradients, optimized tesseroid formulas related to a local left-handed Cartesian coordinate system are used (Grombein et al. 2013):

$$\frac{\partial^2 V(x_1, x_2, x_3)}{\partial x_i \, \partial x_j} = G\rho \int_{\lambda_1}^{\lambda_2} \int_{\varphi_1}^{\varphi_2} \int_{r_1}^{r_2} \left(\frac{3 \Delta x_i \, \Delta x_j}{\ell^5} - \frac{\delta_{ij}}{\ell^3} \right) \mathrm{d}\Omega^*, \tag{2}$$

where $i, j \in \{1, 2, 3\}$, $\mathrm{d}\Omega^* = r'^2 \cos\varphi' \mathrm{d}r' \mathrm{d}\varphi' \mathrm{d}\lambda'$ denotes the spherical volume element, and

$$\Delta x_1 = r' \left[\cos\varphi \sin\varphi' - \sin\varphi \cos\varphi' \cos\left(\lambda' - \lambda\right) \right], \tag{3}$$

$$\Delta x_2 = r' \cos\varphi' \sin\left(\lambda' - \lambda\right), \tag{4}$$

$$\Delta x_3 = r' \cos\psi - r, \tag{5}$$

$$\cos\psi = \sin\varphi \sin\varphi' + \cos\varphi \cos\varphi' \cos\left(\lambda' - \lambda\right), \quad (6)$$

$$\ell = \sqrt{\Delta x_1{}^2 + \Delta x_2{}^2 + \Delta x_3{}^2}. \quad (7)$$

Note that $\partial^2 V/(\partial x_1 \partial x_1)$ is equivalent with the commonly used abbreviation V_{xx}, $\partial^2 V/(\partial x_1 \partial x_2)$ with V_{xy}, and so on.

As the integration with respect to λ' and φ' in Eq. (2) cannot be solved in an analytical way, a second-order approximation is performed using a Taylor series expansion of the integral kernels in combination with a subsequent term-wise integration (Heck and Seitz 2007). Numerical evaluations of Eq. (2) are presented in detail in Grombein et al. (2013). Although the tesseroid formulas are given in spherical approximation, the individual tesseroid bodies are arranged on the surface of the ellipsoid of revolution GRS80 approximating MSL (Moritz 1980).

2.1 Topographic Model

To represent the topographic masses, the $5' \times 5'$ global digital terrain model DTM2006.0 is used (Pavlis et al. 2007). It provides information on surface elevation, ocean and lake depth, as well as ice thickness. Moreover, each grid element of this DTM is classified into one of the six terrain types: (1) dry land above MSL, (2) lake or pond, (3) ocean, (4) grounded glacier, (5) oceanic ice shelf, (6) dry land below MSL. Being superior to conventional modelling approaches, in which the DTM height is used to characterize topographic masses with constant density, the suggested concept relies upon the newly developed and more sophisticated Rock–Water–Ice (RWI) decomposition model.

As schematically illustrated in Fig. 2, each of the DTM2006.0 terrain types consists of a rock, water, and ice proportion, which allows a separate modelling of these masses with variable density values. In this context, the information from DTM2006.0 is exploited to construct a more appropriate $5' \times 5'$ three-layer terrain and density model. Each grid element contains a rock (R), water (W), and ice (I) component with different MSL-heights of the top surface (h_R, h_W, h_I) and thickness (t_R, t_W, t_I). Furthermore, layer-specific density values (ρ_R, ρ_W, ρ_I), as shown in Fig. 2, are derived considering the DTM2006.0 terrain types. Corresponding to this RWI model, the topographic masses are represented by three tesseroid bodies per grid element.

2.2 Isostatic Concept

For the computation of isostatic reductions, the isostatic compensation masses have to be quantified. Using classical isostatic concepts, the distribution of these masses is usually calculated directly from the topographic load by applying the mass equality condition with respect to a particular compensation depth T. The Airy–Heiskanen isostatic scheme, originally related to topographic masses with constant density (Heiskanen and Moritz 1967, p. 135ff), is adapted to the RWI concept using layer-specific density values.

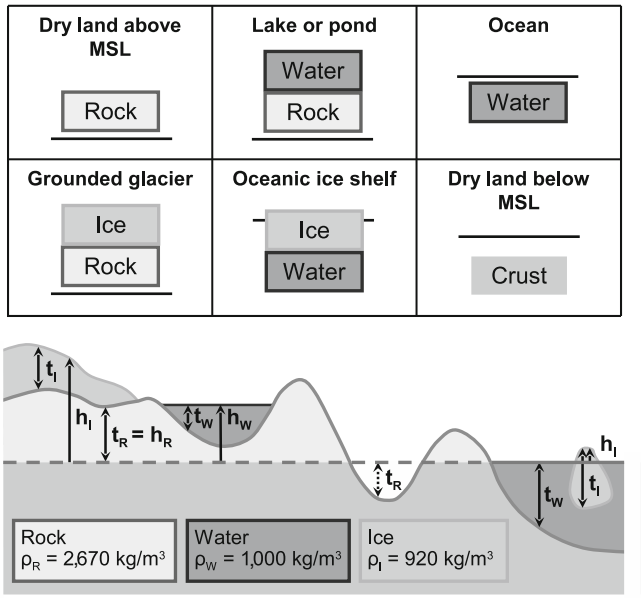

Fig. 2 Schematic presentation of the three-layer RWI model

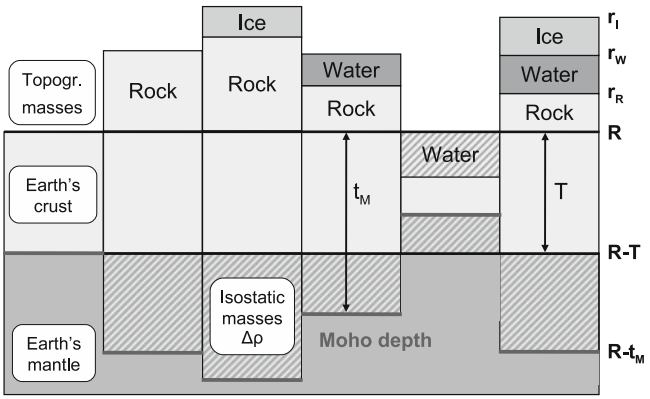

Fig. 3 Schematic presentation of the mod. Airy–Heiskanen concept

Further attempts are made to extend the existing concept by introducing a depth model for the Mohorovičić discontinuity (Moho). To modify the classical Airy–Heiskanen model, the commonly used (anti-)root depths are replaced by Moho depths t_M, fixing the geometry of the isostatic masses. By modification, however, the mass equality condition is no longer be fulfilled. As a consequence, Janák et al. (2012) found that the resulting topographic–isostatic reductions possess large magnitudes contaminating the intended smoothing effect on gravity gradients. In order to satisfy the mass equality condition, the crust-mantle density contrast $\Delta\rho$ is set variable in the following (see Fig. 3). In spherical

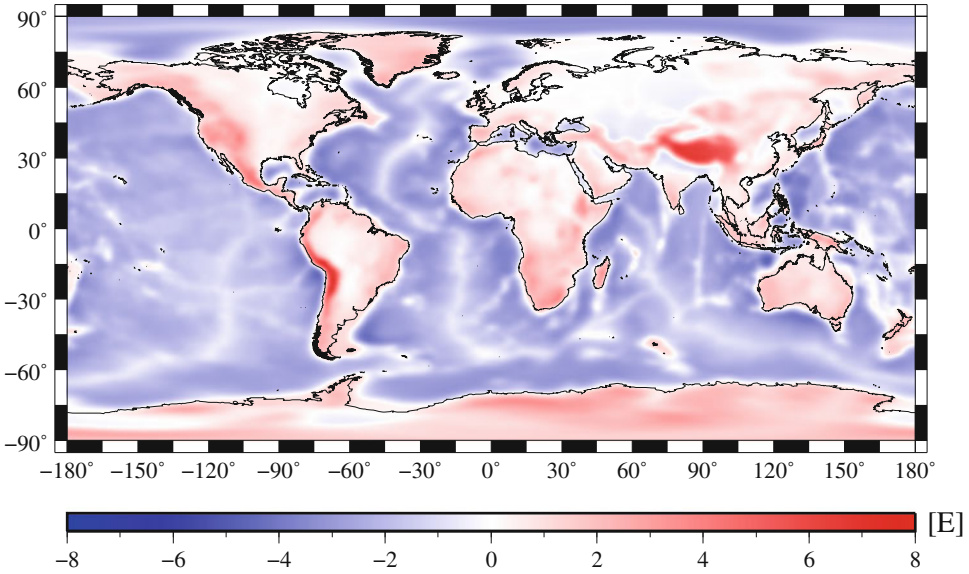

Fig. 4 Topographic reduction values in the radial–radial gravity gradient component V_{zz} at the mean satellite altitude of GOCE

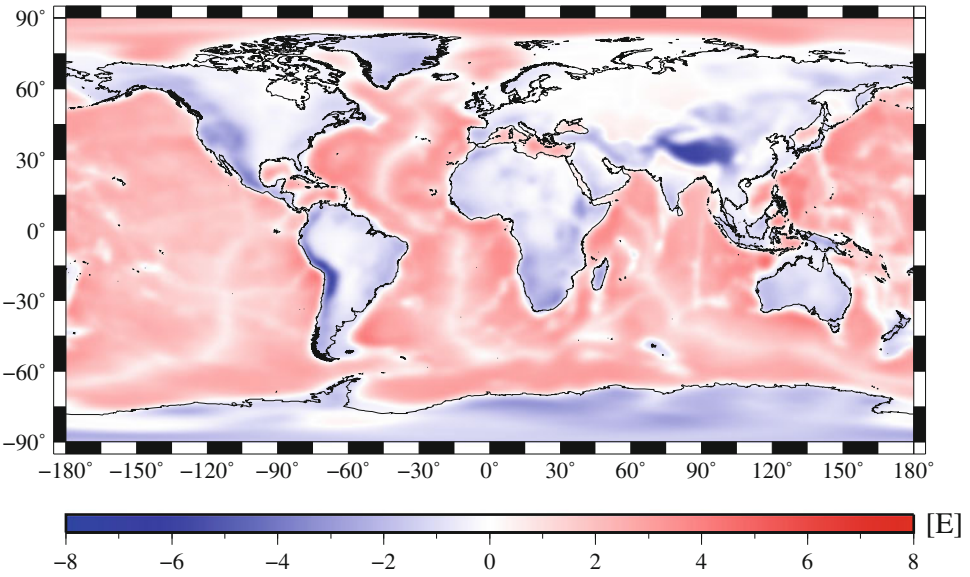

Fig. 5 Isostatic reduction values in the radial–radial gravity gradient component V_{zz} at the mean satellite altitude of GOCE

approximation, the mass equality condition for the RWI approach ($m_{\mathrm{ISO}} = m_{\mathrm{R}} + m_{\mathrm{W}} + m_{\mathrm{I}}$) is given by

$$\Delta\rho \int_{R-t_{\mathrm{M}}}^{R-T} r'^2 \mathrm{d}r' = \rho_{\mathrm{R}} \int_{R}^{r_{\mathrm{R}}} r'^2 \mathrm{d}r' + \rho_{\mathrm{W}} \int_{r_{\mathrm{R}}}^{r_{\mathrm{W}}} r'^2 \mathrm{d}r' + \rho_{\mathrm{I}} \int_{r_{\mathrm{W}}}^{r_{\mathrm{I}}} r'^2 \mathrm{d}r',$$

where R denotes the mean Earth radius and $(r_{\mathrm{R}}, r_{\mathrm{W}}, r_{\mathrm{I}})$ are the geocentric distances of the top surfaces of each layer, i.e. $r_{\mathrm{R}} = R + h_{\mathrm{R}}$, $r_{\mathrm{W}} = R + h_{\mathrm{W}}$, $r_{\mathrm{I}} = R + h_{\mathrm{I}}$. For each grid element the crust-mantle density contrast can then be calculated by

$$\Delta\rho = \frac{\rho_{\mathrm{R}} \left(r_{\mathrm{R}}^3 - R^3\right) + \rho_{\mathrm{W}} \left(r_{\mathrm{W}}^3 - r_{\mathrm{R}}^3\right) + \rho_{\mathrm{I}} \left(r_{\mathrm{I}}^3 - r_{\mathrm{W}}^3\right)}{(R-T)^3 - (R-t_{\mathrm{M}})^3}. \quad (8)$$

In order to accommodate the isostatic information to the topographic model, a $5' \times 5'$ grid model of smoothed global Moho depths is derived from the $2° \times 2°$ global CRUST 2.0 model (Bassin et al. 2000) by means of harmonic analysis and synthesis (Wittwer et al. 2008). The obtained Moho depths are incorporated into the modified Airy–Heiskanen model with respect to a compensation depth of $T = 31$ km.

3 Numerical Investigations

3.1 Reduction Values in GOCE Satellite Altitude

To get an impression of the magnitude of the reduction values, Figs. 4–6 show the radial-radial gravity gradient

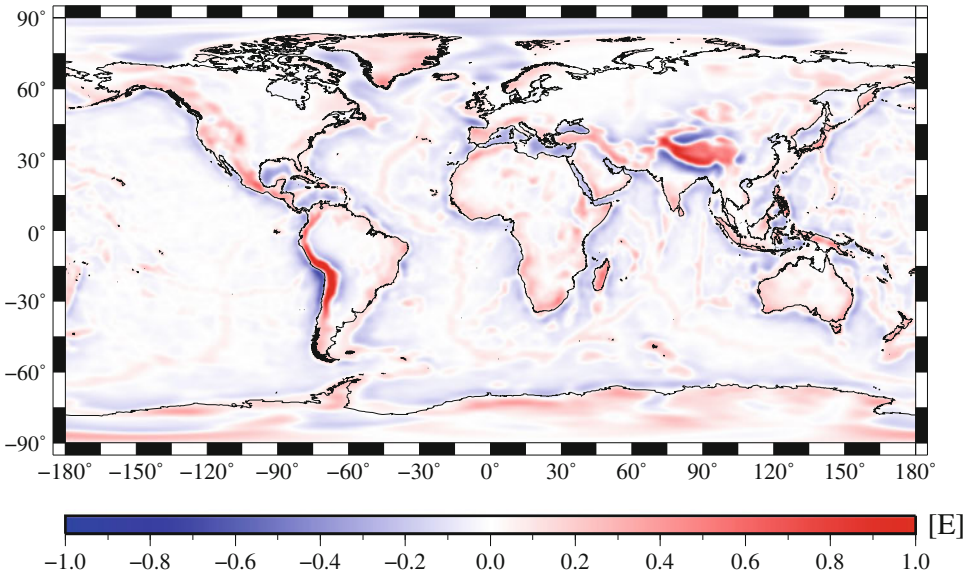

Fig. 6 Topographic–isostatic reduction values in the radial–radial gravity gradient component V_{zz} at the mean satellite altitude of GOCE

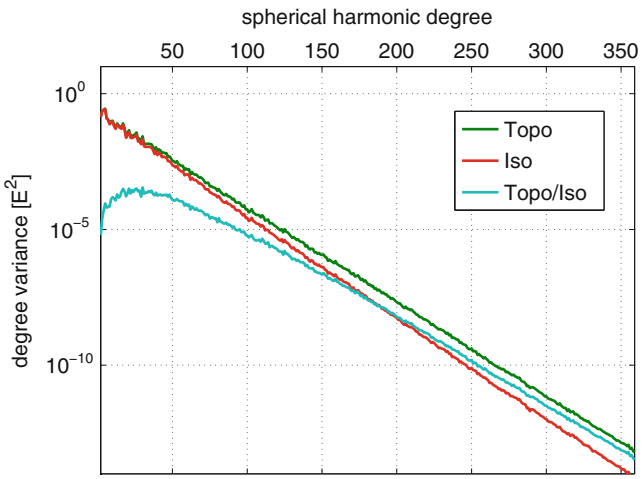

Fig. 7 Degree variances for the reduction values in the radial–radial gravity gradient component V_{zz}

component V_{zz} at the mean satellite altitude of GOCE ($h = 254.9$ km). Topographic and isostatic reductions reach extreme values of about ± 8 E, respectively, which is particularly obvious in the Himalaya region. Both reductions largely cancel each other out, so that the combined topographic–isostatic reduction values are nearly one order of magnitude smaller and about ± 1 E. In Fig. 7 the V_{zz} spectra of the reductions in terms of degree variances is shown. As can be expected, the influence of the isostatic reduction (Iso) is mainly regional showing a decreasing effect on the combined topographic–isostatic reduction (Topo/Iso) with increasing spherical harmonic degree.

3.2 Analysis of the Smoothing Potential

To quantify the smoothing potential, the proposed reduction concept is applied to one week of real GOCE observations collected from October 27 to November 2, 2010. Topographic–isostatic reductions are calculated along the orbit of the GOCE satellite using the measurement positions as computation points. Since the huge amount of 13.6 million reduction values have to be determined, techniques of parallel computing are used to reduce the total computation time to about 4 h by occupying 560 processors (Intel Xeon 2.53 GHz) on the high-performance computer systems hc3 operated at the Karlsruhe Institute of Technology. Before matching the reduction values with the GOCE measurements, they are transformed from the local left-handed system into the Gradiometer Reference Frame.

It should be noted that within the presented topographic–isostatic reduction concept only the high and mid-frequency signal components of the GOCE observations are smoothed, since numerical instabilities are especially attributed to these signal components. The GOCE gradiometer is particularly sensitive within a frequency range of 5–100 mHz, the so-called measurement bandwidth (MBW). However, the observed gravity gradients contain all measured spectral information, also including long-wavelength signals below the MBW. These signals implicate maximum amplitudes of 2,500 E in the V_{zz} component that range in a totally different order of magnitude compared to the reduction values in Fig. 6. To demonstrate the impact of smoothing in the high and mid-frequency components, the GOCE gravity gradient signal content before and after

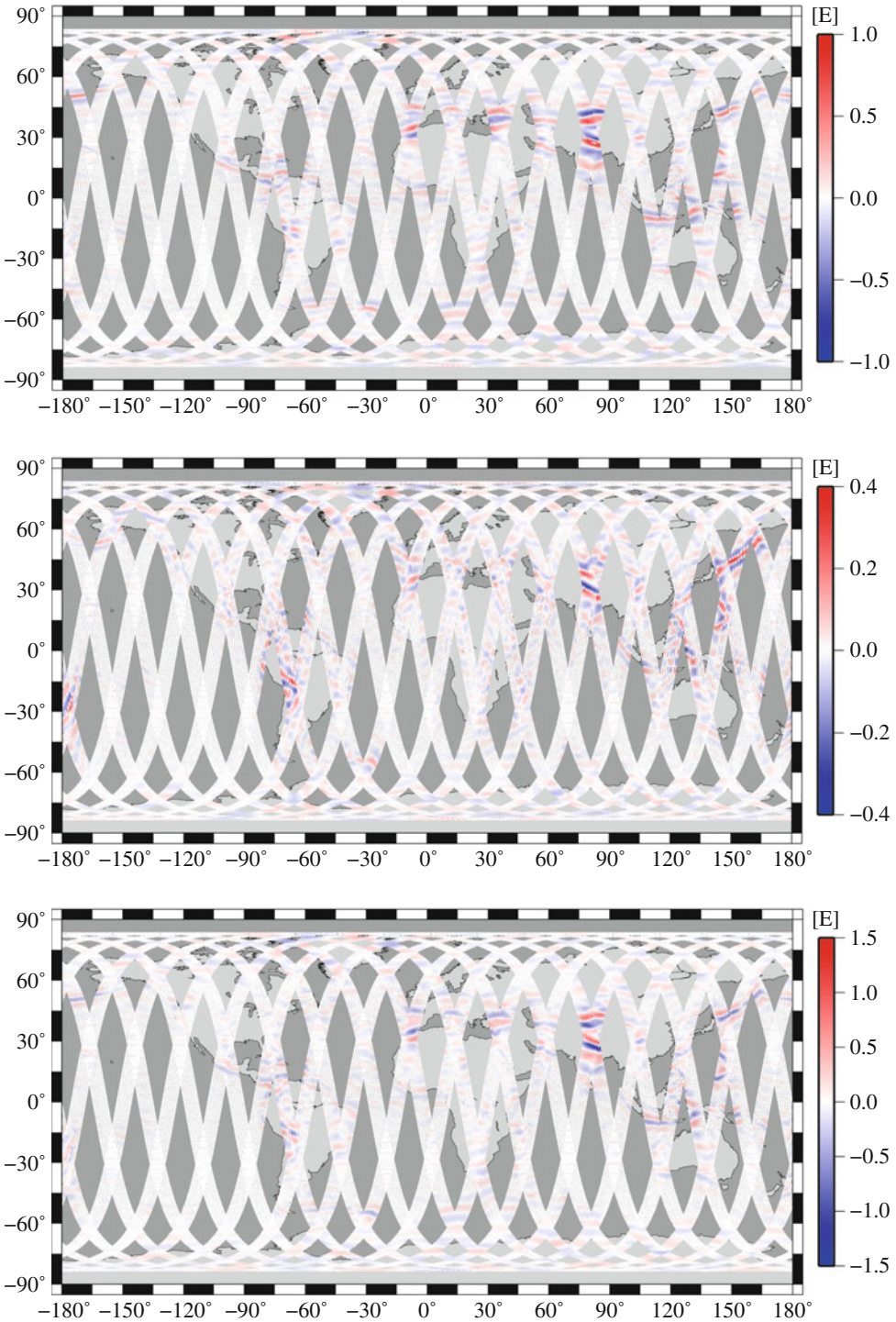

Fig. 8 Original GOCE gradient signals within the MBW (*top*: V_{xx}; *middle*: V_{yy}; *bottom*: V_{zz})

reduction is compared within the MBW. In order to extract the signal content within the bandwidth of interest, a symmetric non-recursive bandpass filter has been applied to the original GOCE gravity gradients as well as to the topographically–isostatically reduced results. In this way, the filtered measurements are strongly detrended and possess the same order of magnitude as the topographic–isostatic reductions.

In Figs. 8 and 9 the original and reduced GOCE gradient signals within the MBW are visualized for V_{xx}, V_{yy}, V_{zz}. Comparing the original and reduced signals with each other, it can be realized that the smoothing effects exhibit region-dependent characteristics and are strongly influenced by the actual topography crossed by the satellite. Significant smoothing effects are detected in regions with highly variable topography, for example the Himalaya in V_{xx} and V_{zz} or

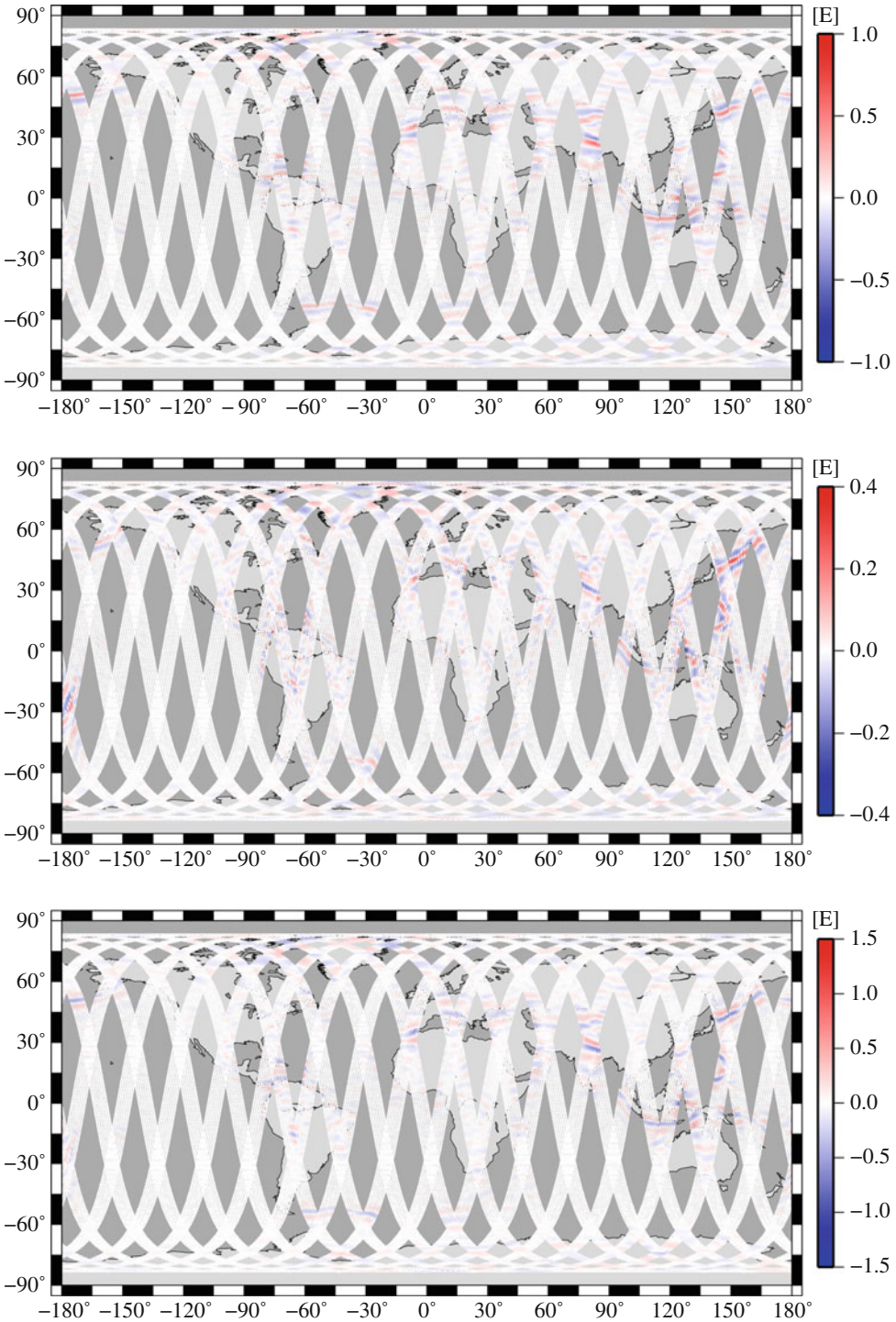

Fig. 9 Topographically–isostatically reduced GOCE gradient signals within the MBW (*top*: V_{xx}; *middle*: V_{yy}; *bottom*: V_{zz})

the Andes in V_{yy}. In contrast, other areas seem to remain uncompensated, for instance the Japan Trench in V_{yy}. Therefore, the use of topographic–isostatic reductions seems particularly suitable for regional applications.

To quantify the degree of smoothing, the percentage changes in standard deviation and range before and after reduction are presented in Table 1. For V_{xx}, V_{yy}, V_{zz}, and V_{xz} the standard deviations, can be reduced by about 30 %. Significant percentage changes in range are found in the V_{xx}, V_{zz}, and V_{xz} components with amounts of about 40 %. In terms of V_{yy} only about 20 % range reduction is visible, which may be explained by the smaller signal amplitude in comparison with the other gradient components. Regarding the components V_{xy} and V_{yz}, only an insignificant smoothing effect is detectable. These two off-diagonal tensor elements are observed less accurately by the GOCE gradiometer. The

Table 1 Percentage changes $[P]$ in standard deviation and range before and after reduction within the MBW

[%]	V_{xx}	V_{yy}	V_{zz}	V_{xy}	V_{xz}	V_{yz}
P_{std}	31.8	27.7	31.5	0.7	31.5	0.7
P_{range}	43.1	22.0	40.4	3.4	43.8	0.0

corresponding signal content in the MBW is superposed by high-frequency noise making smoothing by means of topographic–isostatic reductions not feasible.

4 Conclusions and Outlook

To mitigate the numerical instability in processing the observed GOCE gravity gradients, a smoothing concept based on topographic–isostatic reductions obtained from forward modelling has been presented in this paper. Being advantageous over previous approaches, a new reduction procedure has been suggested which is based on a three-layer Rock–Water–Ice topographic decomposition with variable density values. Geometry and density information is derived from the global topographic data base DTM2006.0. Additionally, a modified Airy–Heiskanen model has been applied, which is improved by incorporating a Moho depth model obtained from the global crust model CRUST 2.0 in combination with the derivation of local density contrasts between crust and mantle. The mass discretization is performed using tesseroid bodies arranged on the surface of the GRS80 ellipsoid.

Numerical results obtained from processing one week of real GOCE measurements show significant smoothing effects on the V_{xx}, V_{yy}, V_{zz}, and V_{xz} gradient components within the gradiometer measurement bandwidth. The degree of smoothing quantified by assessing changes in standard deviations amounts to about 30 %, while the range can be reduced by 20–40 %. Generally, the smoothing effect strongly depends on the variability of the topography crossed by the satellite. This dependence makes the proposed procedure particularly suitable for regional applications. However, for the two less accurately observed components V_{xy} and V_{yz}, the suggested processing strategy seems to be not suitable due to the high-frequency noise in the original gradient measurements.

Further research work will concentrate on the improvement of the reduction concept by means of a more detailed mass-density distribution model. Apart from the suggested smoothing strategy in the space domain, alternative techniques in the frequency domain and other smoothing approaches based on Residual Terrain Modelling, for instance, will be analyzed and compared in the near future.

The current version of the global Rock–Water–Ice topographic–isostatic gravity field model in terms of spherical harmonic coefficients up to degree and order 1800 can be downloaded at http://www.gik.kit.edu/rwi_model.php.

Acknowledgements This research was funded by the German Federal Ministry of Education and Research under grant number 03G0726F within the REAL GOCE project of the GEOTECHNOLOGIEN Programme. The authors would like to thank N.K. Pavlis for providing the global topographic data base DTM2006.0. Furthermore, N. Sneeuw and three anonymous reviewers as well as the Editor-in-Chief are acknowledged for their valuable comments which improved this paper.

References

Anderson EG (1976) The effect of topography on solutions of Stokes' problem. Unisurv S-14, Rep, School of Surveying, University of New South Wales, Australia

Bassin C, Laske G, Masters G (2000) The current limits of resolution for surface wave tomography in North America. EOS Trans AGU 81:F897

Forsberg R, Tscherning CC (1997) Topographic effects in gravity field modelling for BVP. In: Sansò F, Rummel R (eds) Geodetic boundary value problems in view of the one centimeter geoid. Lecture notes in earth sciences, vol 65. Springer, Berlin, pp 239–272. doi:10.1007/BFb0011707

Grombein T, Seitz K, Heck B (2010) Untersuchung zur effizienten Berechnung topographischer Effekte auf den Gradiententensor am Fallbeispiel der Satellitengradiometriemission GOCE. Rep 7547, KIT Scientific Reports. KIT Scientific Publishing, Karlsruhe. doi:10.5445/KSP/1000017531

Grombein T, Seitz K, Heck B (2013) Optimized formulas for the gravitational field of a tesseroid. J Geod 87(7):645–650. doi:10.1007/s00190-013-0636-1

Heck B, Seitz K (2007) A comparison of the tesseroid, prism and point-mass approaches for mass reductions in gravity field modelling. J Geod 81:121–136. doi:10.1007/s00190-006-0094-0

Heiskanen WA, Moritz H (1967) Physical geodesy. W. H. Freeman & Co., San Francisco

Janák J, Wild-Pfeiffer F (2010) Comparison of various topographic–isostatic effects in terms of smoothing gradiometric observations. In: Sansò F, Mertikas SPP (eds) IAG symposia, vol 135. Springer, Berlin, pp 377–381. doi:10.1007/978-3-642-10634-7_50

Janák J, Wild-Pfeiffer F, Heck B (2012) Smoothing the gradiometric observations using different topographic–isostatic models: a regional case study. In: Sneeuw et al (eds) Proc. VII Hotine-Marussi symposium, Rome, Italy, 2009. IAG symposia, vol 137. Springer, Berlin, pp 245–250. doi:10.1007/978-3-642-22078-4_37

Moritz H (1980) Geodetic reference system 1980. Bull Géod 54:395–405. doi:10.1007/BF02521480

Pavlis N, Factor J, Holmes S (2007) Terrain-related gravimetric quantities computed for the next EGM. In: Kiliçoğlu A, Forsberg R (eds) Proceedings of the 1st international symposium IGFS: gravity field of the earth, Istanbul, Turkey, 2006, Harita Dergisi, Special Issue 18, pp 318–323

Wild F, Heck B (2008) Topographic and isostatic reductions for use in satellite gravity gradiometry. In: Xu et al (eds) Proc. VI Hotine-Marussi symposium, Wuhan, China, 2006. IAG symposia, vol 132. Springer, Berlin, pp 49–55. doi:10.1007/978-3-540-74584-6_8

Wild-Pfeiffer F (2008) A comparison of different mass elements for use in gravity gradiometry. J Geod 82:637–653. doi:10.1007/s00190-008-0219-8

Wittwer T, Klees R, Seitz K, Heck B (2008) Ultra-high degree spherical harmonic analysis and synthesis using extended-range arithmetic. J Geod 82:223–229. doi:10.1007/s00190-007-0172-y